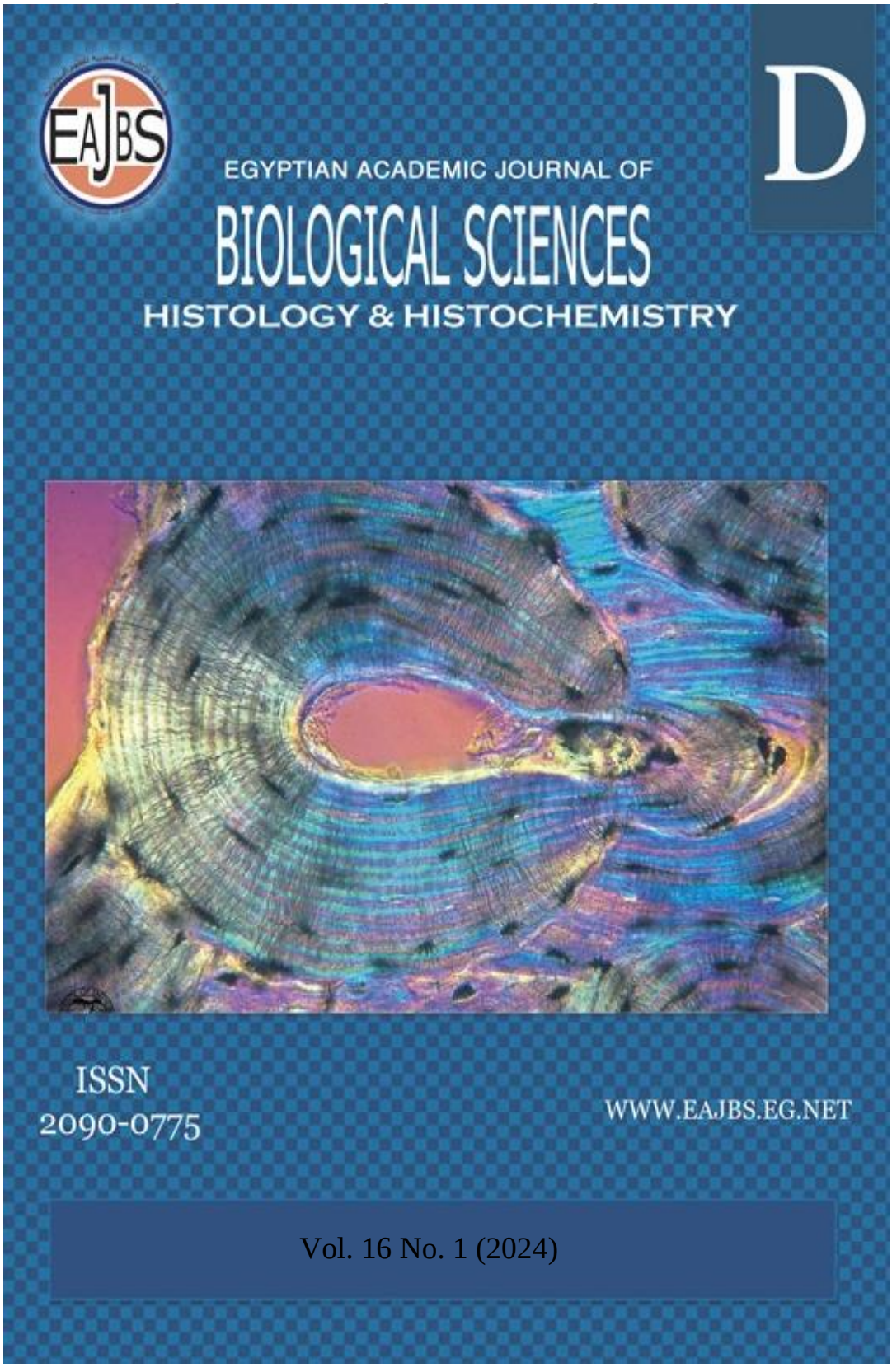

Citation: Egypt. *Acad. J. Biolog. Sci. (D-Histology and histochemistry) Vol.16(1) pp 11-26(2024)*
DOI: 10.21608/EAJBSD.2024.336980

Egypt. Acad. J. Biolog. Sci., 16(1): 27-40 (2024)

Egyptian Academic Journal of Biological Sciences
D. Histology & Histochemistry
ISSN 2090 – 0775
http://eajbsd.journals.ekb.eg

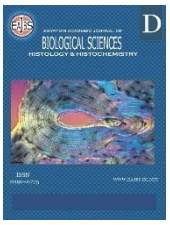

Effects of Acetylsalicylic Acid on the Gastric Mucosa and the Possible Ameliorative Role of Silymarin in Adult Albino Rat

Reneah R. Bushra and Ashraf E. Bastwrous
Department of Human Anatomy and Embryology, Faculty of Medicine, Assiut University.
***E-mail:** reneah@aun.edu.eg ; ashrafedward@aun.edu.eg

ARTICLE INFO
Article History
Received:16/9/2023
Accepted: 17/1/2024
Available:21/1/2024

***Keywords*:**
Gastric mucosa, ASA, Silymarin, Rat.
.

ABSTRACT

Background: Aspirin or acetylsalicylic acid (ASA) is among the most popular used drugs in the world. Gastric lesions are one of aspirin's often-occurring side effects. Silymarin is a natural compound that exhibits effects against inflammation, oxidation, and apoptosis. **Aim of the work:** This study was conducted to evaluate ASA-induced gastric mucosal damage and the potential ameliorative role of silymarin.

Material and Methods: Thirty adult male albino rats were randomly divided into three equal groups: a control group (subdivided into a negative control group without any medication and a positive control group that received distilled water/day orally by gastric gavage for 2 weeks), ASA-treated group (received 200 mg ASA/kg b.w./day orally for 2 weeks), and ASA+silymarin-treated group (received 200 mg ASA/kg b.w./day in addition to 50 mg silymarin/kg b.w./day, orally for 2 weeks). At the end of the experiment, the rats were anaesthetized and sacrificed. The stomach was removed, opened, and processed for histological and iNOS immunohistochemical evaluation. Area % of collagen fibres and iNOS immune expression and gastric mucosal thickness of all animal groups were measured and compared.

Results: The ASA induced gastric mucosal histological changes in the form of erosion, degeneration, vacuolization of cells, and dilatation of blood capillaries. The area % of collagen fibres and iNOS was significantly increased and gastric mucosal thickness was significantly decreased in ASA-treated groups in comparison to the control. These changes were improved in the ASA+silymarin-treated group. **Conclusion:** ASA induced gastric mucosal injuries and the concomitant administration of silymarin could ameliorate these effects.

INTRODUCTION

One of the most crucial tissues of the body is the mucosa of the stomach due to its role but it has the potential for diseases (Meyer, 2018). Gastric mucosal injury is one of the most widespread problems in the world. When the stomach's defense systems are altered, the gastric mucosa may undergo changes that eventually lead to erosion and subsequent ulceration (Zou *et al.*, 2021).

Gastric erosion usually occurs due to an imbalance between the gastric mucosal defensive and aggressive factors.

Aggressive factors include pepsin, hydrochloric acid, non-steroidal anti-inflammatory drugs (NSAIDs), ethanol, and helicobacter pylori. Local defensive factors include protective agents such as Epidermal Growth Factors, prostaglandins, mucus secretion, bicarbonate, cellular regeneration, and blood flow (Narayanan *et al.,* 2018 and Galura *et al.,* 2019).

Acetylsalicylic acid (ASA) is an old medication known as aspirin and is frequently used to prevent and treat cerebrovascular disorders (Desborough and Keeling, 2017). ASA is one of the NSAIDs that is frequently used to treat rheumatoid arthritis and associated conditions as well as to avoid cardiovascular thrombotic disorders (Heibashy *et al.,* 2014).

The reactive oxygen species play a key role in the development of stomach erosion. As a result, different regimens of reactive oxygen metabolite scavengers seem to be brand-new therapeutic approaches for digestive illnesses (Bhattacharyya *et al.,* 2014). In contrast to the harmful effects of chemicals, interest has been sparked in employing natural molecules extracted from plants (Szymanska *et al.,* 2017).

One of the most traditional and widely used medicinal herbs for their beneficial effects on the liver and other organs is the milk thistle (Silybum marianum) (Gillessen and Schmidt, 2020). This plant is indigenous to the Mediterranean region and is common throughout North America and Europe. Additionally, it is grown in Australia, China, Iran, India, Africa, and South America (Abenavoli *et al.,* 2018).

A polyphenolic flavonoid known as silymarin is extracted from the milk thistle (Khalili *et al.,* 2009). It is a mixture of bioflavonoids including silybin, silydianin, isosilybin, and silychristin that can be found in the fruit, seeds, and leaves of this plant (Karimi *et al.,* 2011). Silymarin has been used clinically either alone or as a major component of various pharmaceutical preparations for centuries as a hepatoprotective agent and has exhibited protective effects against inflammation, oxidation, and apoptosis (Avci *et al.,* 2016).

Considering the biological activities presented by silymarin and its widespread use as herbal medicine, the present study aimed to evaluate the ameliorative effect of silymarin against acetylsalicylic acid-induced gastric mucosal injury in adult albino rats.

MATERIAL AND METHODS

Chemicals:

Acetylsalicylic acid was used in its commercially available formulation as Rivo tablets; each tablet contained 320 mg ASA; Arab Pharma & Chemical Mfg Co., Egypt. Five tablets containing 1600 mg ASA were diluted in 40 ml distilled water. So, each 1ml distilled water would contain 40 mg ASA. A dose of 200 mg ASA/kg body weight (b.w.)/day was given via gastric gavage. Silymarin sachets were obtained from SEDICO Pharmaceutical Company and dissolved in distilled water.

Experimental Design:

Thirty adult male albino rats 3 months old (200-250gm) were used and randomly divided into three equal groups (10 rats, each):

Group 1 (control group): was subdivided equally into a negative control group without any medication and a positive control group that received distilled water/day orally by gastric gavage for 2 weeks.

Group 2 (ASA-treated group): was given 200 mg ASA/kg b.w./day orally by gastric gavage for 2 weeks according to D'Argenio *et al.* (2008).

Group 3 (ASA+silymarin-treated group): was given 200 mg ASA/kg b.w./day orally by gastric gavage in addition to 50 mg silymarin/kg b.w. orally by gastric gavage for two weeks according to Girish *et al.* (2009).

At the end of the experiment, all groups were sacrificed under inhalational anaesthesia with ether. Their abdomens were opened in the middle and the

stomach was removed, opened along the greater curvature, and gently rinsed with saline. Thereafter, some stomach fundus specimens were fixed in neutral formalin and stained by Haematoxylin & Eosin (H&E) and Masson's trichrome. Immunohistochemical evaluation with inducible nitric oxide synthase (iNOS), which is a marker for oxidative stress, was also performed. Other specimens were immersed in 5% glutaraldehyde, stained by Toluidine blue and processed for the scanning and transmission electron microscopic studies.

The mean ± standard deviation (SD) of the mean of the area percentage (%) of the collagen fibres and iNOS immune expression of all groups was detected. Also, the mean gastric mucosal thickness (the perpendicular distance between the gastric mucosal surface and the muscularis mucosa in the H&E-stained slides) was measured. Ten different captured non-overlapping fields in Masson's trichrome and iNOS-immune-stained slides at X400 and H&E-stained slides at X100 of five rats of each group were obtained. Image J software (National Institute of Health, USA Java 1.8.0-66) was used to analyze the photographed fields**.**

All collected data were statistically analyzed by the SPSS program version 21 (SPSS Inc., Chicago, IL, USA) using one-way analysis of variance (ANOVA) and post-hoc test. Data were expressed as mean ± SD and p-values equal to or less than 0.05 were considered significant.

RESULTS

A) Histological Results:

A.I. Light Microscopic Results:

A.I.1. Haematoxylin and Eosin Stain:

The stomach of the control adult rat revealed that the gastric wall was composed of mucosa, submucosa, and muscle layer. The mucosa was separated from the submucosa by muscularis mucosa and exhibited numerous gastric pits, regularly arranged tightly packed tubular glands, lamina propria and, blood capillaries. The gastric mucosa was lined by spherical parietal cells with acidophilic cytoplasm and central vesicular rounded nuclei and distributed through the length of the glands. Chief cells with basal nuclei and basal basophilic cytoplasm were noticed. Mucous cells having flattened basal nuclei and vacuolated cytoplasm were observed (Figs. 1a, 1d).

The stomach of the ASA-treated group showed dilatation of the gastric pits, erosion of the gastric mucosa with disorganization of adjacent glandular architecture, marked reduction of the glandular thickness, vacuolation of cells, dilatation of the gastric glands and congestion of the blood capillaries. The parietal cells revealed rarified cytoplasm and faint nuclei. The chief cells exhibited vacuolated cytoplasm and the mucous cells had pyknotic nuclei (Figs. 1b, 1e, inset).

The stomach of the ASA+silymarin-treated group showed intact tubular glands with gastric pits, lamina propria, muscularis mucosa, submucosa, muscle layer, and moderately dilated and congested blood capillaries. The parietal, chief and mucous cells were intact (Figs. 1c, 1f).

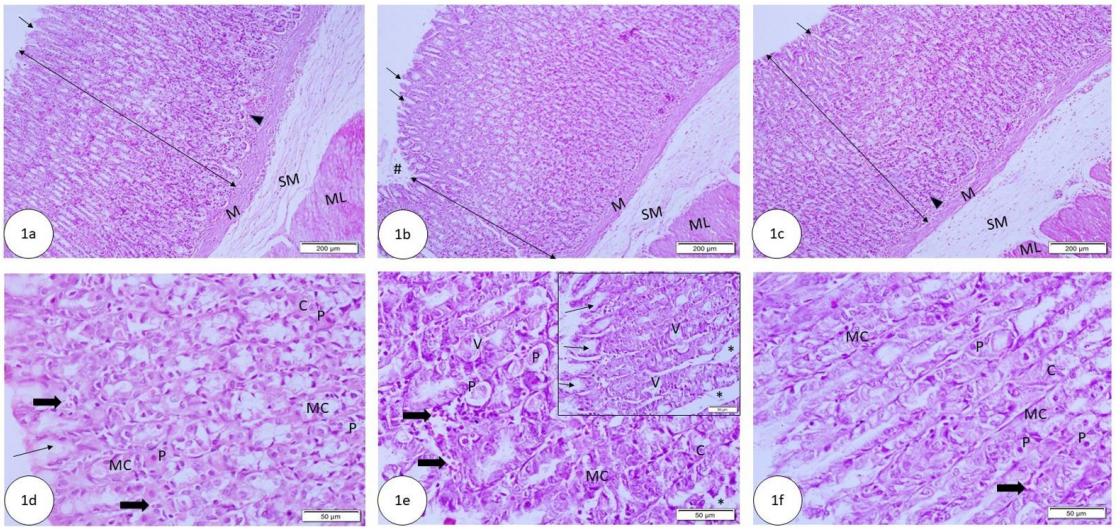

Plate 1: Photomicrographs of the rat gastric fundic mucosa of the studied groups. The control group shows regularly arranged tightly packed tubular glands (↕) with gastric pits (thin arrow), lamina propria (▲), muscularis mucosa (M), submucosa (SM), muscle layer (ML), blood capillaries (thick arrows), spherical parietal cells (P) with acidophilic cytoplasm and rounded central vesicular nuclei, chief cell (C) with basal nuclei and basal basophilic cytoplasm and mucous cells (MC) having flattened basal nuclei and vacuolated cytoplasm **[Figs. 1a,1d]**. The ASA-treated group shows dilatation of the gastric pits (thin arrows), erosion of the gastric mucosa with disorganization of adjacent glandular architecture (#), marked reduction of the glandular thickness (↕), vacuolation of cells (v), dilated congested blood capillaries (thick arrows), dilated gastric glands (*), parietal cells (P) with rarified cytoplasm and faint nuclei, chief cells (C) with vacuolated cytoplasm and mucous cells (MC) with pyknotic nuclei. Notice the muscularis mucosa (M), submucosa (SM) and muscle layer (ML) [**Figs. 1b,1e, inset]**. The ASA+silymarin-treated group shows retained glandular thickness (↕), gastric pits (thin arrow), lamina propria (▲), muscularis mucosa (M), submucosa (SM), muscle layer (ML), blood capillaries (thick arrows), parietal cells (P), chief cells (C) and mucous cells (MC**) [Figs. 1c,1f]**. [H&E: 1a-1c; X100, 1d-1f, inset; X400, respectively]

A.I.2. Toluidine Blue Stain:

The gastric mucosa of the control adult rats showed a normal gastric mucosa with gastric pits, intact blood capillaries, parietal cells, chief cells, and mucous cells (Fig. 2a). The gastric mucosa of the ASA-treated group showed dilated gastric pits, dilated and congested blood capillaries, vacuolated parietal and chief cells, and degenerated mucous cells (Fig. 2b). The ASA+silymarin-treated group showed less dilated gastric pits and blood capillaries. The parietal, chief and mucous cells appeared intact (Fig. 2c).

A.I.3. Masson's Trichrome Stain:

The stomach wall of the control adult rats showed a minimal amount of collagen fibres in the muscularis mucosa, submucosa, and between bases of gastric glands (Fig. 2d). The stomach wall of the ASA-treated group showed a great amount of collagen fibres in the muscularis mucosa, submucosa and between bases of gastric glands (Fig. 2e). The stomach wall of the ASA+silymarin-treated group showed a moderate amount of collagen fibres in the submucosa and lamina propria (Fig. 2f).

A.I.4. Immunohistochemical Results:

The gastric mucosal cells of the control rats group showed a weak immune reactivity to iNOS (Fig. 2g). The mucosal cells of the ASA-treated group showed a strong positive immune reaction to iNOS (Fig. 2h). The ASA+silymarin-treated group showed a moderate immune reaction to iNOS (Fig. 2i).

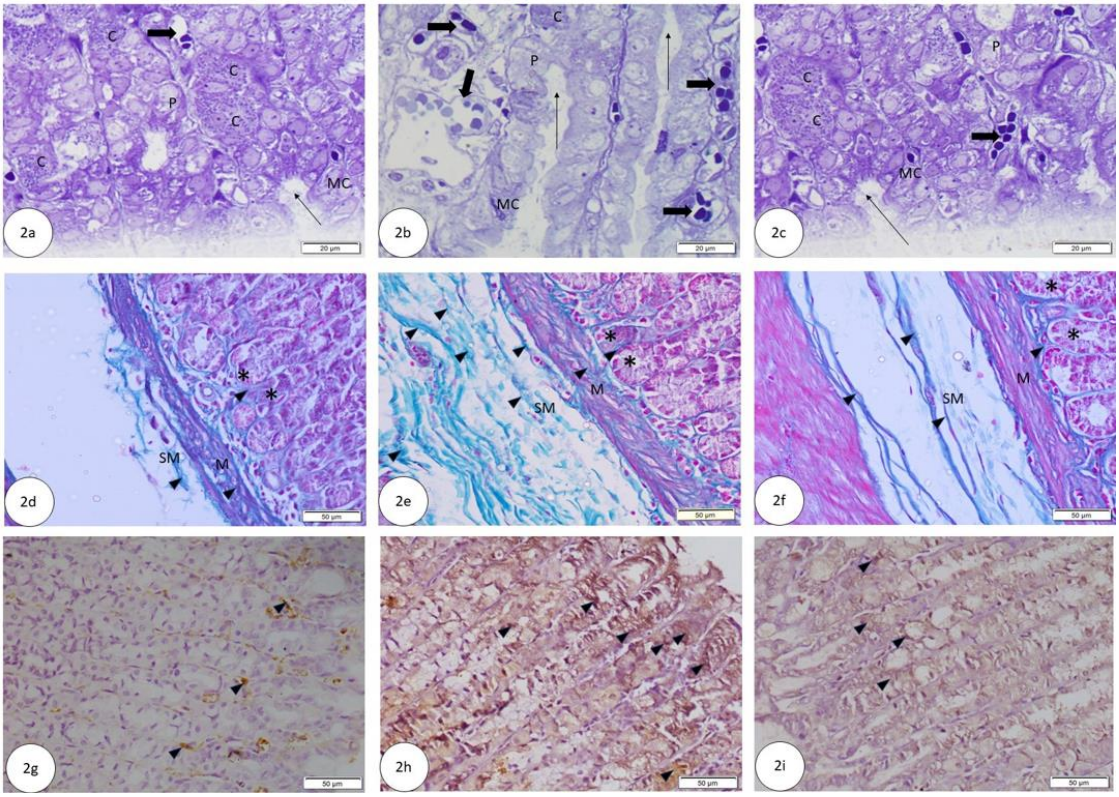

Plate 2: Photomicrographs of the rat gastric fundic mucosa of the studied groups. The control group shows normal gastric mucosa with gastric pits (thin arrow), intact blood capillaries (thick arrow), parietal cells (P), chief cells (C), and mucous cells (MC) **[Fig. 2a]**, a minimal amount of collage fibres (arrowheads) in the muscularis mucosa (M), submucosa (SM), and between bases of gastric glands (*) **[Fig. 2d]** and a weak immune reaction to iNOS (arrowheads) **[Fig. 2g].** The ASA-treated group shows dilated gastric pits (thin arrows), dilated and congested blood capillaries (thick arrows), vacuolated parietal (P) and chief (C) cells, and degenerated mucous cells (MC) **[Fig. 2b]**, a great amount of collagen fibres (arrowheads) in the muscularis mucosa (M), submucosa (SM), and between bases of gastric glands (*) **[Fig. 2e]** and a strong immune reaction to iNOS (arrowheads) **[Fig. 2h].** The ASA+silymarin-treated group shows less dilated gastric pits (thin arrow), residual congested blood capillaries (thick arrow), intact parietal cells (P), chief cells (C), and mucous cells (MC) **[Fig. 2c]**, a moderate amount of collage fibres (arrowheads) in the muscularis mucosa (M), submucosa (SM), and between bases of gastric glands (*) **[Fig. 2f]** and a moderate immune reaction to iNOS (arrowheads) **[Fig. 2i]**. [Toluidine blue: 2a-2c; X1000, Masson's trichrome: 2d-2f; X400, iNOS immune-stain: 2g-2i; X400, respectively]

A. II. Electron microscopic results:

A.II.1. Scanning electron microscopy:

The gastric mucosa viewed from the lumen of the control adult rats revealed a sheet of intact cells with a cobblestone appearance and mucosal ropes extending from the gastric pits (Figs. 3a, 3d). The gastric mucosa of the ASA-treated group showed mucosal erosions, disruption of the gastric mucosal cells, and destruction of the mucus layer (Figs. 3b, 3e). The gastric mucosa of the ASA+silymarin-treated group revealed a sheet of intact gastric mucosal cells and mucus extending from the gastric pits (Figs. 3c, 3f).

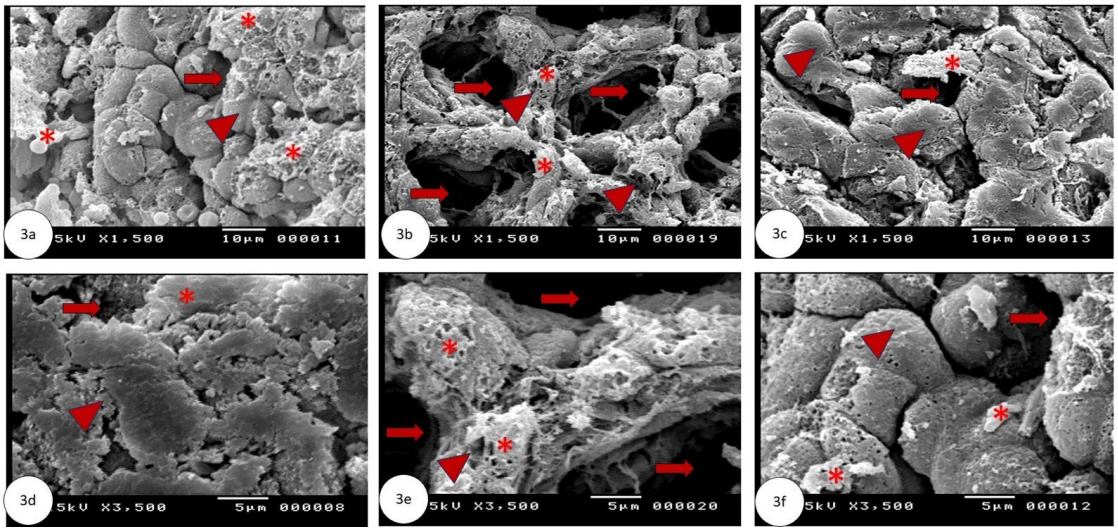

Plate 3: Scanning electron photomicrographs of the gastric mucosa viewed from the lumen of the different studied groups. The control group shows a sheet of intact gastric mucosal cells with a cobblestone appearance (▲) with gastric pits (arrow) and ropes of mucus (*) extending from gastric pits **[Figs. 3a, 3d]**. The ASA-treated group shows mucosal erosions (arrows), disruption of the gastric mucosal cells (▲), and destruction of the mucus layer (*) **[Figs. 3b, 3e]**. The ASA+silymarin-treated group shows gastric pits (arrow), a sheet of intact gastric mucosal cells (▲), and mucus (*) extending from the gastric pits **[Figs. 3c, 3f]**. [SEM: 3a-3c; X1500, 3d-3f; X3500, respectively]

A.II.2. Transmission electron microscopy:

The control parietal cells contained rounded nuclei, numerous electron-dense mitochondria, Golgi apparatus, ribosomes, cytoplasmic vacuoles, tubulovesicles, and intracellular canaliculi lined by numerous microvilli (Fig. 4a). The parietal cells of the ASA-treated group showed irregularly outlined nuclei, swollen mitochondria, cytoplasmic rarefaction and vacuolations, dilated Golgi apparatus, and intracellular canaliculi with destructed microvilli (Fig. 4b). The ASA+silymarin-treated parietal cells showed oval nuclei, electron-dene mitochondria, cytoplasmic vacuoles, tubulovesicles, and intracellular canaliculi lined by intact microvilli (Fig. 4c).

The chief cells of the control group showed basal rounded nucleus, packed cisternae of rough endoplasmic reticulum, apical zymogenic secretory granules, Golgi apparatus, and mitochondria (Fig. 4d). Whereas, the chief cells of the ASA-treated group revealed heterochromatic indented nuclei, markedly dilated rough endoplasmic reticulum, swollen mitochondria and few apical large secretory granules (Fig. 4e). The chief cells of the ASA+silymarin-treated group showed rounded nucleus with a prominent nucleolus, apical zymogenic secretory granules, rough endoplasmic reticulum, and Golgi apparatus (Fig. 4f).

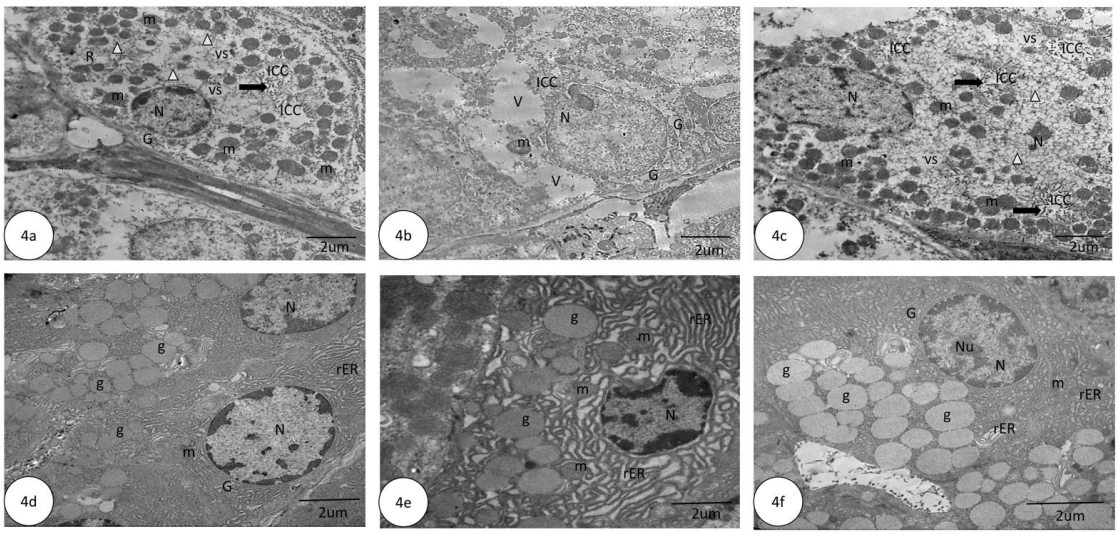

Plate 4: TEM photomicrographs of the parietal cells **[Figs. 4a-4c]** and chief cells **[Figs. 4d-4f]** of the gastric glands of the studied groups. A control parietal cell shows a rounded nucleus (N), numerous electron-dense mitochondria (m), Golgi apparatus (G), ribosomes (R), cytoplasmic vacuoles (Δ), tubulovesicles (VS) and intracellular canaliculi (ICC) lined by numerous microvilli (arrow) **[Fig. 4a]**. An ASA-treated parietal cell shows an irregularly outlined nucleus (N), swollen mitochondria (m), cytoplasmic rarefaction and vacuolations (V), dilated Golgi apparatus (G), and intracellular canaliculi (ICC) with destructed microvilli **[Fig. 4b]**. An ASA+silymarin-treated parietal cell shows an oval nucleus (N), many electron-dene mitochondria (m), cytoplasmic vacuoles (Δ), tubulovesicles (VS) and intracellular canaliculi (ICC) lined by intact microvilli (arrows) **[Fig. 4c]**. Two adjacent control chief cells show basal rounded nuclei (N), packed cisternae of rough endoplasmic reticulum (rER), mitochondria (m), Golgi apparatus (G), and apical zymogenic secretory granules (g) **[Fig. 4d]**. An ASA-treated chief cell shows a heterochromatic indented nucleus (N), markedly dilated rough endoplasmic reticulum (rER), swollen mitochondria (m), and few apical large secretory granules (g) **[Fig. 4e]**. An ASA+silymarin-treated chief cell shows a rounded nucleus (N) with a prominent nucleolus (Nu), Golgi apparatus (G), mitochondria (m), rough endoplasmic reticulum (rER), and apical zymogenic secretory granules (g) **[Fig. 4f]**. [TEM; X 4800]

The enteroendocrine cells of the control group had oval nuclei that were located in a deeply enfolded envelope and exhibited a prominent nucleolus. The cytoplasm contained rough endoplasmic reticulum, free ribosomes, basally located dense spherical granules (each being enveloped with a loose-fitting membrane), Golgi complex located beside the nucleus and small spherical mitochondria with hardly visible mitochondrial ridges (Fig. 5a). The enteroendocrine cells of the ASA-treated group revealed pyknotic heterochromatic irregular nuclei, swollen mitochondria, cytoplasmic vacuolations, rarified cytoplasm and dense secretory granules (Fig. 5b). The enteroendocrine cells of the ASA+silymarin-treated group revealed rounded nuclei with a prominent nucleolus, secretory granules, Golgi apparatus, mitochondria, rough endoplasmic reticulum, and free ribosomes (Fig. 5c).

The control mucous-secreting cells revealed a basally located oval nucleus with a prominent nucleolus, Golgi complexes located beside the nucleus, a lot of mucoid secretory granules bordering the lumen of the stomach, mitochondria, and rough endoplasmic reticulum (Fig. 5d). The mucous-secreting cells of the ASA-treated group showed shrunken hyperchromatic nuclei, dilated Golgi, swollen mitochondria and mucoid secretory granules (Fig. 5e). In the ASA+silymarin-treated group, the

mucous-secreting cells contained basally located oval nuclei showing residual hyperchromatic state, Golgi complex located beside the nucleus, mitochondria and mucoid secretory granules bordering the lumen of the stomach (Fig. 5f).

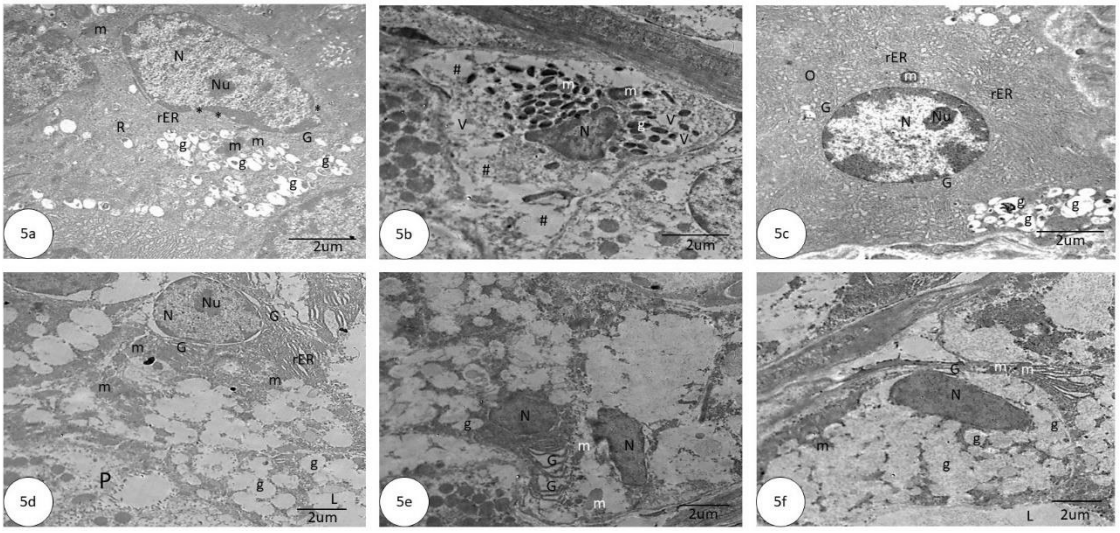

Plate 5: TEM photomicrographs of the enteroendocrine cells **[Figs. 5a-5c]** and mucous-secreting cells **[Figs. 5d-5f]** of the gastric glands of the examined groups. A control enteroendocrine cell shows an oval nucleus (N) located in a deeply enfolded envelop (*) with a prominent nucleolus (Nu), rough endoplasmic reticulum (rER), free ribosomes (R), numerous dense spherical granules basally located each being enveloped with loose-fitting membrane (g), Golgi complex (G) located beside the nucleus and small spherical mitochondria (m) with hardly visible mitochondrial ridges **[Fig. 5a]**. An ASA-treated enteroendocrine cell shows a pyknotic heterochromatic irregular nucleus (N), swollen mitochondria (m), cytoplasmic vacuolations (V), rarified cytoplasm (#) and dense secretory granules (g) **[Fig. 5b]**. An ASA+silymarin-treated enteroendocrine cell shows a rounded nucleus (N) with a prominent nucleolus (Nu), Golgi apparatus (G), free ribosomes (O), mitochondria (m), secretory granules (g), and rough endoplasmic reticulum (rER) **[Fig. 5c]**. A mucous-secreting cell of the control group shows a basally located oval nucleus (N) with a prominent nucleolus (Nu), Golgi complex (G) located beside the nucleus, a lot of mucoid secretory granules (g) bordering the lumen (L) of the stomach, mitochondria (m) and rough endoplasmic reticulum (rER). Notice the adjacent parietal cell (P) **[Fig. 5d]**. Two adjacent mucous-secreting cells of the ASA-treated group show shrunken hyperchromatic nuclei (N), dilated Golgi (G), swollen mitochondria (m) and mucoid secretory granules (g) **[Fig. 5e]**. A mucous-secreting cell of the ASA+silymarin-treated group shows a basally located oval nucleus (N) with residual hyperchromatin, Golgi complex (G) located beside the nucleus, mitochondria (m), and mucoid secretory granules (g) bordering the lumen (L) of the stomach **[Fig. 5f]**. [TEM: 5a-5c; X 7200, 5d-5f; X 4800, respectively]

B) Morphometric Results:

The statistical analysis of the morphometric measurements of the different examined groups revealed a significant increase in the mean area % of the collagen fibres and iNOS immune expression in the gastric mucosa of the ASA-treated group compared to the control. The mean area % of collagen fibres and iNOS immune expression of the ASA+silymarin-treated group showed non-significant change compared to the control one (Table 1& Histogram 1).

On the other hand, there was a significant decrease in the gastric mucosal thickness of the ASA-treated group compared to the control group. The gastric mucosal thickness of the ASA+silymarin-treated group showed a non-significant change compared to the control group (Table 2& Histogram 2).

Table 1: The means of the area percentage of collagen fibres by Masson's Trichrome staining and iNOS immune expression of the different groups.

	group 1 control group (mean±SD)	group 2 ASA-treated group (mean±SD)	group 3 ASA+silymarin-treated group (mean±SD)	p-value
Area % of collagen fibres	30.83±1.47	69.2±4.76***	33.2±1.48	0.000
Area % of iNOS immune expression	0.52±0.02	7.58±0.37***	0.66±0.03	0.000

Data are presented as mean ± SD
(*): Significant as compared to control

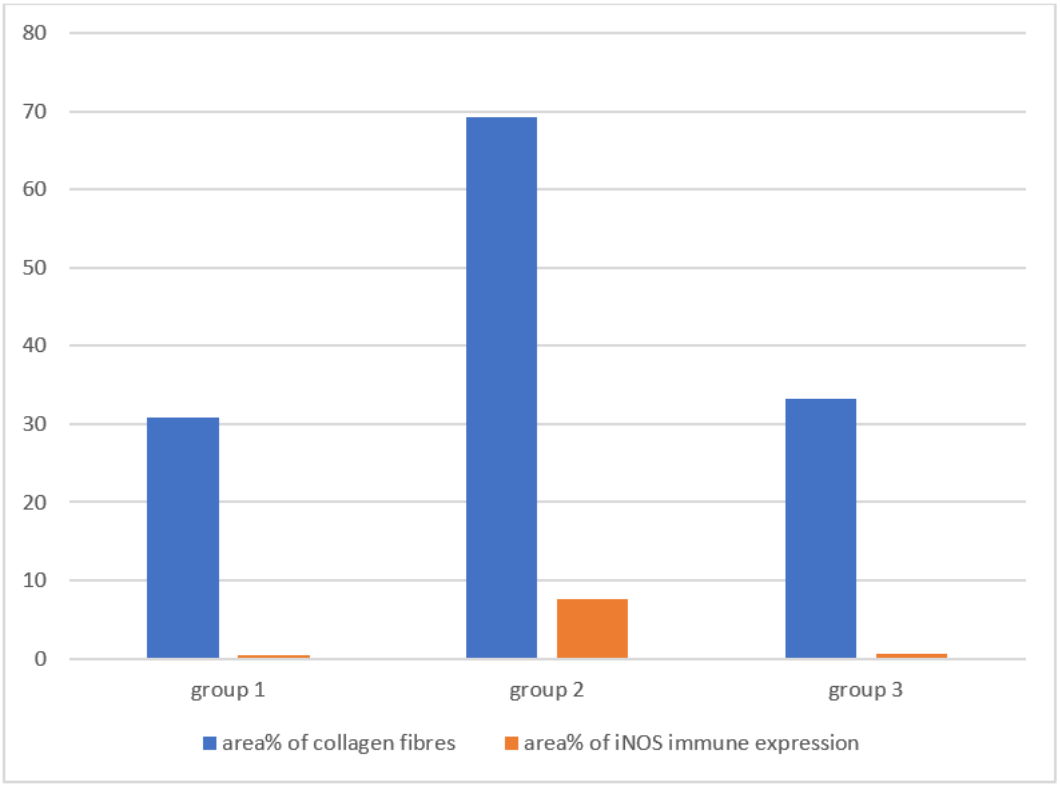

Histogram 1: Showing means of the area percentage of collagen fibres and iNOS immune expression of the different studied groups.

Table 2: The means of the gastric mucosal thickness of the different groups.

	group 1 control group (mean±SD)	group 2 ASA-treated group (mean±SD)	group 3 ASA+silymarin-treated group (mean±SD)	p-value
Gastric mucosal thickness (um)	954.8±3.11	607.4±5.59***	946±6.51	0.000

Data are presented as (mean ± SD)
(*): Significant as compared to control

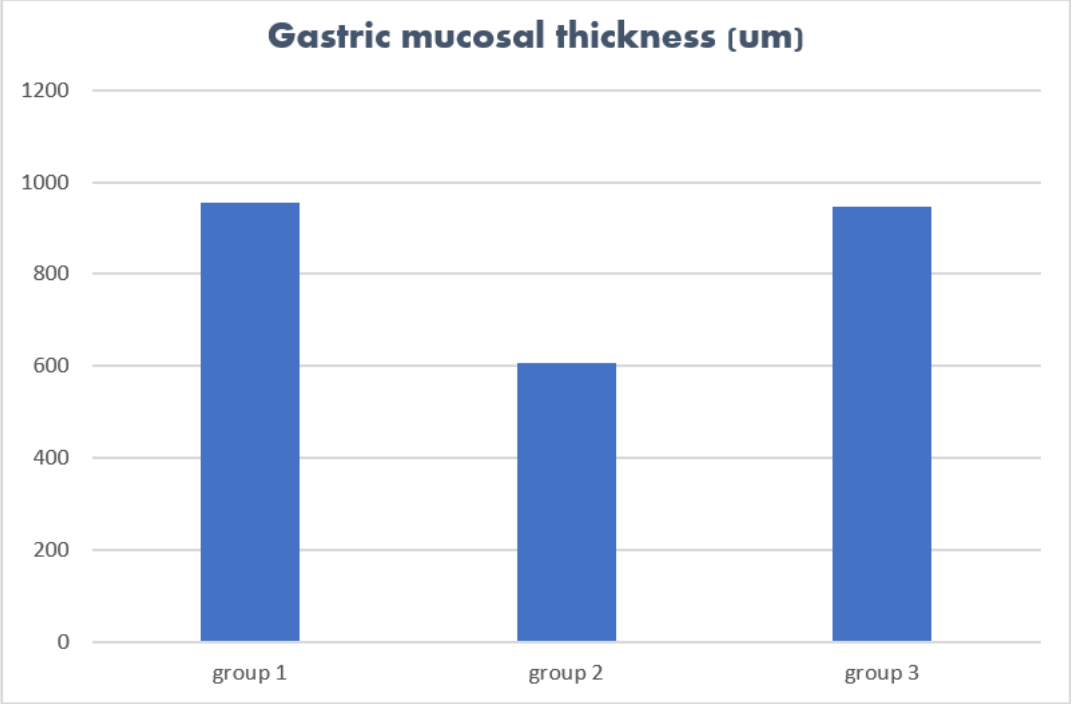

Histogram 2: showing the means of the gastric mucosal thickness of the different groups.

DISCUSSION

Gastric mucosal injuries are common gastrointestinal disorders (Yousaf *et al.*, 2014). In the present study, the administration of ASA caused histological disturbances of the gastric mucosa observed by light microscopy and came parallel with the scanning and electron microscopic results. ASA in the present work induced discontinuity of the gastric mucosa, disorganization of the glandular architecture, vacuolation of cells and dilated gastric glands. These findings were in accordance with Majeed *et al.* (2015), Salga *et al.* (2017), and Mahmoud and Abd El-Ghffar (2019) who demonstrated that the administration of salicylates resulted in a loss of gastric mucosal integrity, eroded surface epithelial cells, submucosal oedema, and inflammatory cell infiltration.

The observed findings could be explained by Papatheodoridis and Archimandritis (2005) and Matsui *et al.* (2011) who attributed the local direct damage of the gastric mucosa by unionized salicylic acid in gastric juice that entered and accumulated within the gastric epithelial cells then became ionized intracellularly. It disturbed cell metabolic functions, increased mucosal permeability and allowed the back diffusion of H+ ions. Yang *et al.* (2017) stated that ASA released TNF-α and IL-6 and caused oxidative injury via Glutathione depletion and myeloperoxidase induction. Moreover, Takeuchi (2012) stated that gastric mucosal injury arose primarily from the inhibition of COX-1 which was constitutively expressed and generated prostaglandins involved in the maintenance of the integrity of the gastric mucosa. However, it was reported that COX-1 and COX-2 either alone or in concert contributed to gastric mucosal defense. They added that there was also evidence that only blockade of both COX-1 and COX-2 carried a major risk of gastric ulceration.

The present work revealed that ASA caused a reduction of the glandular thickness and this finding was confirmed morphometrically. This observation was in agreement with Mahmoud and Abd El-Ghffar (2019). This finding could be explained by the loss and destruction of

the gastric mucosal cells and the erosion caused by ASA administration.

The current study revealed that ASA induced capillary congestion and dilatation. These results are in accordance with Zhang *et al.* (2014) who demonstrated that aspirin caused congestion and haemorrhagic gastric erosion, and glandular vacuolation. In addition, the congestion of blood vessels described in this study was in agreement with Bayramli and Ulutas (2008) who observed hemorrhagic erosions, dilatation, and congestion of the nearby blood vessels after administration of a single oral dose of 200 mg aspirin /kg body weight.

The electron microscopic results of the ASA-treated group of the present work revealed the destruction of the parietal, chief, mucous and enteroendocrine cells. Hagras *et al.* (2014) and Shalaby *et al.* (2016) reported that disrupted canaliculi and the appearance of dense bodies were signs of parietal cells' early damage. Shalaby *et al.* (2016) reported that intracellular canaliculi disruption and dilatation lead to parietal cell vacuolization. Moreover, Polat *et al.* (2011) suggested that damage to the tight junction permeability between the gastric mucosal epithelial cells may be implicated in induced chief cells disorder.

The present study revealed an excessive amount of collagen fibres deposited in the submucosa and lamina propria of the ASA-treated group and this observation was confirmed morphometrically. Kumar *et al.* (2003) attributed the increased collagen deposition at sites of inflammation to the growth factors elaborated by the attracted inflammatory mononuclear cells to the sites of injury. In addition, Hagras *et al.* (2014) observed the same finding after treatment with the anti-rheumatic drug Leflunomide. Pochetuhen *et al.* (2007) reported the close interrelation between cellular infiltration and fibrosis and clearly explained the associated increased deposition of collagen fibres by the activated fibroblasts which were depicted hand in hand with the cellular infiltration.

Regards the immunohistochemical results, the present study exhibited that ASA caused a strong positive immune reaction to iNOS and this observation was confirmed morphometrically as there was a significant increase in the area % of iNOS in the ASA-treated group. This finding was in agreement with Konturek *et al.* (2006) who reported that one of the mechanisms by which aspirin could damage the gastric mucosa was via the increased NO production due to iNOS over-expression.

The present study demonstrated an ameliorative effect of silymarin against salicylate-induced gastric mucosal injury. These results agreed with those of Huilgol and Jamadar (2012) and Surai (2015) who demonstrated that silymarin has significant anti-ulcerative activity by dual mechanisms; the ability to decrease the HCl secreted by gastric glands and a cytoprotective action by prevention of peroxidative processes which in turn lead to increases in the endogenous antioxidants levels.

In addition, a possible mechanism for the cytoprotective action of silymarin was that silymarin stimulated DNA-dependent RNA polymerase, leading to increased protein synthesis and thus promoting reparative and healing processes as observed by Khazaei *et al.* (2022).

According to Eraky *et al.* (2018), silymarin also has antifibrotic, anticancer, and anti-inflammatory properties. In addition to preserving redox equilibrium, silymarin could lower NO, lactate dehydrogenase, and reactive oxygen species levels as stated by Chtourou *et al.* (2010). By preserving the integrity of mitochondrial activity, silymarin could also suppress the mitochondrial apoptotic pathway as reported by Fernández-Moriano *et al.* (2015). Moreover, Anahita *et al.* (2020) reported that silymarin had improved the tissue indicators of wound healing in

experimental models of full-thickness gastric wounds in rats.

Conclusion: Salicylates induce gastric mucosal injuries and fortunately the concomitant administration of silymarin could ameliorate these effects.

Ethical Statements: This study was carried out in strict accordance with the International Guidelines for the Care and Use of Laboratory Animals. The experimental protocol was approved by the Ethics Committee at the Faculty of Medicine, Assiut University, Assiut, Egypt (Approval number: IRB17300823).

Conflet of Interest: The authors declare no conflict of interest.

Authors Contributions:I hereby verify that all authors mentioned on the title page have made substantial contributions to the conception and design of the study, have thoroughly reviewed the manuscript, confirm the accuracy and authenticity of the data and its interpretation, and consent to its submission.

Funding: No funding was received.

REFERENCES

Abenavoli L, Izzo AA, Milić N, Cicala C, Santini A, Capasso R, 2018. Milk thistle (Silybum marianum): A concise overview on its chemistry, pharmacological, and nutraceutical uses in liver diseases. *Phytotherapy Research,* 32(11):2202-2213.

Anahita PH, Mehdi B, Aliasghar T, 2020. Effect of Oral Administration of Silymarin on Healing Full-thickness Gastric Wound in Rats. *Majallah-i Dānishgāh-i ʻUlūm-i Pizishkī-i Qum Qom University of Medical Sciences journal*; 14(8):10-20.

Avci H, Tunca R, Epikmen ET, Birincioğlu SS, Sekkin SB Murat, Akşit H, 2016. Protective and antigenotoxic effects of Silymarin and Curcumin in experimental cyclophosphamide intoxication in rats. *Kafkas Universitesi Veteriner Fakultesi Dergisi;* 22:693–701.

Bayramli G, Ulutas B, 2008. Acute phase protein response in dogs with experimentally induced gastric mucosal injury. *Veterinary Clinical Pathology;* 37:312–316.

Bhattacharyya A, Chattopadhyay R, Mitra S, Crowe SE, 2014. Oxidative stress: an essential factor in the pathogenesis of gastrointestinal mucosal diseases. *Physiological Reviews* ;94(2):329-354.

Chtourou Y, Fetoui H, Sefi M, 2010. Silymarin, a natural antioxidant, protects cerebral cortex against manganese- induced neurotoxicity in adult rats. *Biometals;* 23(6):985–996.

D'Argenio G, Mazzone G, Tuccillo C, Grandone I, Gravina AG, Graziani G, 2008. Apple polyphenol extracts prevent aspirin-induced damage to the rat gastric mucosa. *British Journal of Nutrition;* 100:1228–1236.

Desborough MJ, Keeling DM, 2017. The aspirin story-from willow to wonder drug. *British Journal of Haematology;* 177:674-683.

Eraky SM, El-Mesery M, El-Karef A, 2018. Silymarin and caffeine combination ameliorates experimentally-induced hepatic fibrosis through down-regulation of LPAR1 expression. *Biomedicine & Pharmacotherapy;* 101:49–57.

Fernández-Moriano C, González-Burgos E, Gómez-Serranillos MP, 2015. Mitochondria-targeted protective compounds in Parkinson's and Alzheimer's diseases. *Oxidative Medicine and Cellular Longevity:* 408927.

Galura GM, Chavez LO, Robles A, McCallum R, 2019. Gastroduodenal Injury: Role of Protective Factors. *Current*

Gastroenterology Reports; 21: 34.

Gillessen A, Schmidt HH, 2020. Silymarin as Supportive Treatment in Liver Diseases: A Narrative Review. *Advances in Therapy;* 37(4):1279-1301.

Girish C, Koner BC, Jayanthi S, 2009. Hepatoprotective activity of picroliv, curcumin and ellagic acid compared to silymarin on paracetamol induced liver toxicity in mice. *Fundamental and Clinical Pharmacology;* 23(6):735-745.

Hagras GM, Mansour MA, Ghoneim NS, Damhogy RA, Abdel Aziz SA, 2014. Effect of the Anti-Rheumatic Drug Leflunomide (Avara®) on The Pyloric Region of Stomach of Adult Male Albino Rats and The Possible Protective Effect of Ranitidine (Histological and Histochemical Study). *Journal of American Science;* 10(11).

Heibashy MI, Mazen GM, Ibrahim MA, 2014. Efficacy and Safety of some Medical Herbs on Gastric Ulcer Induced by Aspirin in Rats. *Journal of Pharmacy and Bioallied Sciences;* 9(3): 1927.

Huilgol SV, Jamadar MG, 2012. Silymarin, an antioxidant bioflavonoid, inhibits experimentally -induced peptic ulcers in rats by dual mechanisms. *International Journal of Applied and Basic Medical Research;* 2(1):63-66.

Karimi G, Vahabzadeh M, Lari P, Rashedinia M, Moshiri M, 2011. Silymarin, a promising pharmacological agent for treatment of diseases. *Iranian Journal of Basic Medical Sciences;* 14:308–317.

Khalili M, Hasanloo T, Tabar S, Rahnama H, 2009. Influence of exogenous salicylic acid on flavonolignans and lipoxygenase activity in the hairy root cultures of Silybum marianum. *Cell Biology International;* 33:988–994.

Khazaei R, Seidavi A, Bouyeh M, 2022. A review on the mechanisms of the effect of silymarin in milk thistle (Silybum marianum) on some laboratory animals. *Veterinary Medicine and Science;* 8(1):289-301.

Konturek PC, Kania J, Hahn EG, Konturek JW, 2006. Ascorbic acid attenuates aspirin-induced gastric damage: role of inducible nitric oxide synthase. *Journal of Physiology and Pharmacology*; 57:125-136.

Kumar S, Boehm J, Lee J, 2003. P38 MAP kinases: key signaling molecules as therapeutic targets for inflammatory diseases. *Nature Reviews Drug Discovery;* 2(9):717-726.

Mahmoud YI, Abd El-Ghffar EA, 2019. Spirulina ameliorates aspirin-induced gastric ulcer in albino mice by alleviating oxidative stress and inflammation. *Biomedicine & Pharmacotherapy;* 109:314-321

Majeed WB, Aslam I, Javed KT, Muhammad F, Ali A, Raza A, 2015. Histopathological evaluation of gastro protective effect of Berberis vulgaris (Zereshk) seeds against aspirin induced ulcer in albino mice. *Pakistan Journal of Pharmaceutical Sciences;* 28 1953–1958.

Matsui H, Shimokawa O, Kaneko T, Nagano Y, Rai K, Hyodo I, 2011. The pathophysiology of non_steroidal anti-inflammatory drug (NSAID) induced mucosal injuries in stomach and small intestine. *Journal of Clinical Biochemistry and Nutrition,* 48(2):107-111.

Meyer AR, Goldenring JR, 2018. Injury, repair, inflammation and metaplasia in the stomach. *The*

Journal of Physiology; 596 (17): 3861-3867.

Narayanan M, Reddy KM, Marsicano E, 2018. Peptic Ulcer Disease and Helicobacter pylori infection. *Missouri Medicine;* 115:219-224.

Papatheodoridis GV, Archimandritis AJ, 2005. Role of Helicobacter pylori eradication in aspirin or non-steroidal anti-inflammatory drug users. *World Journal of Gastroenterology;* 11(25): 3811 -3816.

Pochetuhen K, Luzina IG, Lockatell V, Choi J, Todd NW, Atamas SP, 2007. Complex Regulation of Pulmonary Inflammation and Fibrosis by CCL18. *The American Journal of Pathology;* 171(2): 428-437.

Polat B, Albayrak Y, Suleyman B, Dursun H, Odabasoglu F, Yigiter M, Halici Z, Suleyman H, 2011. Antiulcerative effect of dexmedetomidine on indomethacin –induced gastric ulcer in rats. *Pharmacological Reports;* 63: 518-526.

Salga MS, Ali HM, Abdulla MA, Abdelwahab SI, Elhassan T, Yagoub U, 2017. Synthesis and gastroprotective activities of some zinc (II) complexes derived from (E)-2-(1-(2-(piperazin-1-yl) ethylimino) ethyl) phenol and (E)-4-(1-(2 (piperazin-1-yl) ethylimino) ethyl) benzene-1, 3-diol Schiff bases against aspirin induced ulceration. *Arabian Journal of Chemistry;* (10): 1578-1589.

Shalaby SA, Eid EM, Ahmed OF, Abdow MF, 2016. Protective Effect of Ascorbic Acid and Ranitidine on the Indomethacin Induced Gastric Injury in Adult Albino Rats; Light and Electron Microscopy. *International Journal of Clinical and Developmental Anatomy;* 2 (1): 1-13.

Surai PF, 2015. Silymarin as a Natural Antioxidant: An Overview of the Current Evidence and Perspectives. *Antioxidants (Basel);* Mar 20; 4 (1): 204-247.

Szymanska R, Pospisil P, Kruk J, 2017. Corrigendum to Plant-Derived Antioxidants in Disease Prevention. *Oxidative Medicine and Cellular Longevity:* Volume 2017, Article ID 5092754, 1 page.

Takeuchi K, 2012. Pathogenesis of NSAID-induced gastric damage: importance of cyclooxygenase inhibition and gastric hypermotility. *World Journal of Gastroenterology;* 18(18):2147-2160.

Yang CT, Lai ZZ, Zheng ZH, Kang JM, Xian M, Wang RY, Shi K, Meng FH, Li X, Chen L, Zhang H, 2017. A novel pH-controlled hydrogen sulfide donor protects gastric mucosa from aspirin-induced injury. *Journal of Cellular and Molecular Medicine; 21*(10):2441-2451.

Yousaf A, Ali S, Bokhari ZH, Khalid AM, Sheikh MA, 2014. Protective Effect of Vitamin E on Indomethacin Induced Gastric Ulcers. *Journal of Rawalpindi Medical College (JRMC);* 8(2):286-289.

Zhang JY, WU QF, Wan Y, Song SD, Xu J, Xu XS, 2014. Protective role of [23] hydrogen-rich water on aspirin-induced gastric mucosal damage in rats. *World Journal of Gastroenterology;* 20(6): 1614-1622.

Zou Y, Cui X, Xiang Q, Guo M, Liang Y, Qu Y, Yang X, 2021. Protective effect of against ethanol-induced gastric ulcer and its mechanism. Journal of Zhejiang University. *Medical sciences;* 50(5):561-567.